

## HEAT TRANSFER CHARACTERISATION OF COPPER COMPOSITE ALLOYS

Mr. C.D.V Ravi Kumar<sup>1</sup>, Mr. E. Raju<sup>2</sup>, Mr. D. Sreepal<sup>3</sup>

<sup>1,2,3</sup> Assistant Professor, Adithya Engineering College, Kakinada, AP

### Abstract:

Aluminium nanoparticles were added to the Cu–Zn alloy in order to assess their effects on the microstructural, tribological and corrosion characteristics of preparation alloys. A mixture of zero volt percent copper and zinc powders and 5volt  $\alpha$ -Al nano-powder was used for the satellite ball mill alloying. The results showed that after 18 hours of mechanical alloy, the solid solution Cu–Zn had formed. The mechanically alloyed polvo was compacted and the obtained green compacts were fried at 750 ° C for 30 minutes. Nanoparticles were distributed uniformly in the Cu–Zn alloy matrix alumina. The tribology characteristics were evaluated through pin on disks, which showed that after introducing alumina nanoparticles the friction coefficient and wear rate were reduced to 20 percent and 40 percent. The corrosion properties of samples exposed to a NaCl solution of 3.5wt percent were investigated with immersion and potentio dynamic polarization methods.

**Keywords:** nanocomposites; copper zinc alloys; alumina; microstructure; corrosion; wear properties.

### Introduction:

aluminum bronze alloys are coppers, with aluminium as a main alloying element in the range of 5-4% compositionally, and iron, nickel, manganese, silicone and tin are sometimes deliberately introduced other alloying elements which depend on the in-tended application of aluminum bronze bronze. In particular for demanding applications, these make them more preferred "Aluminum bronzes are most appreciated for their high strength and corrosion resilience in a wide range of aggressive media." They are most commonly used in applications in which their resistance to corrosion makes them preferable to other engineering materials. "The copper component of the alloy prevents colonization of marine organisms, including algae, lichens, barnacles and mould, and can thus be used in applications where such colonization is not wanted rather than in stainless steel or another non-cupric alloy.

### Literature review:

**Rajkovicet al. [1]** The Cu and Al<sub>2</sub>O<sub>3</sub> nanocomposites were prepared using two methods and the 800 ° C hot press was followed by sintered. In the first procedure copper powder was mixed with the 2wt aluminum powder and the second method in a ball mill, and 4wt commercial alumina powder was mixed with copper powder.

**Rajković, D. Božić[2]** The study was carried out by the addition of alumina nanoparticles to study the effect of the Cu–Zn alloy on its microstructure as well as tribological and corrosive properties. In a satellite ball mill, copper and zinc powder mixtures were prepared as raw material and then sintered into conventional stove with a volume of 5% and Al<sub>2</sub>O<sub>3</sub> nanopowder. As a raw material.

### Methodology

The microhardness and thermal stability of the copper aluminum specimens are greater that of copper – alumina. The mechanism of Cu–Zn alloy systems with zn contents from 15% to 85% by ball milling has been reported by Pabi and it has been proven that the mechanism of the mechanical alloy process is the continuous diffusion of the mixture, which is first tries the mechanism of electrical conductivity produced by the copper – alumina powder. A zn diffusion into Cu resulted in a solid solution (phases  $\alpha$  and  $\beta$ ) being developed in this respect. The Cu–Al<sub>2</sub>O<sub>3</sub> Nanocomposite was supplemented by ball fraying and sintering at 700-850 ° C. With alumina nanoparticles, the copper matrix was dispersed evenly. The existence and uniform distribution of aluminum nanoparticles as a strong-enhancing agent had a significant impact on the hardness of the samples. Whether the relationship Corrosion, wear and tribology may be affected between the refinement and the metal matrix by a nanocomposite strengthening stage.

### Experimental methods:

For nanocomposites raw substances and Alumina Nano powder of an average particle size of 50 nm, the average copper and zinc powders with less then 20  $\mu$ m were selected. Mechanical fraying cycles have been performed in Cu–40wt per cent Zn, a mixture of 0 Vol per cent and 5 Vol per cent of alumina nanoparticles for mechanical alloys and the effect of introducing alumina nanoparticles. A powder mixing with 1 ml and ethanol as process control agent (PCA) was used mechanical under an argon atmosphere for 18 h, 10 mm (10 mm) and 10 mm (10 mm) balls at the speed. In the satellite ball mill, the ball-to-powder ratio of 1:10. XRD was characterized by powder mechanically alloyed on an X'Pert Philips X-Pert MPD diffractometer co-K $\alpha$  radiation source

(0.154056 nm). The micrographs of beginning powders (SEM (Philips XL30) and the TEM (Zeiss EM10C) characterized the morphology of particles. As shown in this picture, the powder particles of zinc were largely spherical, originally containing copper.

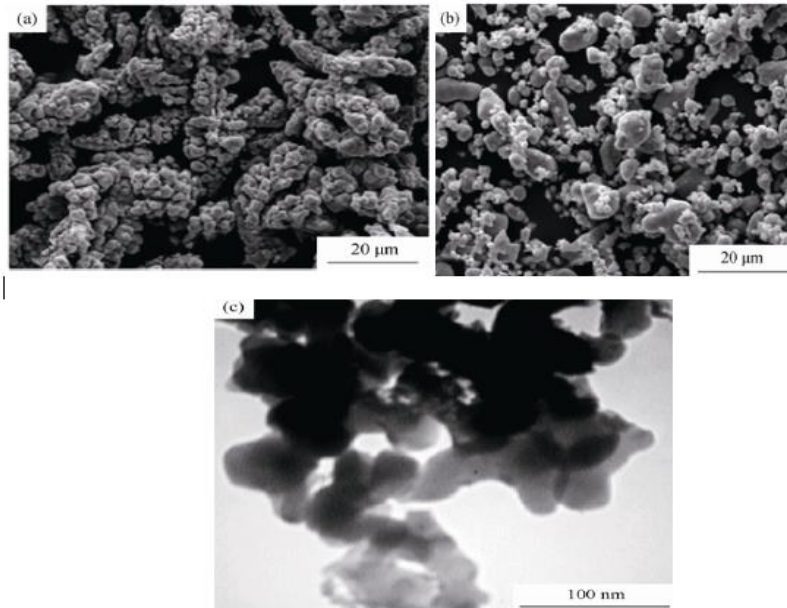


**Figure: SEM image of powder particles of (a) copper and (b) zinc and (c) TEM image of alumina nanoparticles prior to mechanical milling.**

#### X-RAY DIFFRACTION ANALYSIS

Mixture models of XRD Cu<sub>60</sub>Zn<sub>40</sub> powder for various mechanical frying periods. It consists of five phases after four hours of friction: the copper, zinc (CuZn<sub>5</sub>),  $\mu$  phase (Cu<sub>5</sub>Zn<sub>8</sub>) and the  $\alpha$  phase (Cu<sub>0.64</sub>Zn<sub>0.36</sub>). This mixture is made up of powder. Radius of copper and zinc are 0.133 nm, and 0.128 nm, respectively. Diffusion of zinc into a copper grid causes the copper grid parameter to be reduced and the copper top angle to a greater double value. As is clearly shown in the Fig. A solid copper solution (zinc) was found in this connection after 10 hours of frying. Copper and zinc peaks after ten hours of grinding were also not observed in the XRD pattern. All elements increased in maximum width after extending the frying time while subsequently reducing the peak intensity. Alloy occurs in nuclear dimensions, leading to solid solutions, intermetallic composition and even amorphous phases in the mechanical framing process. The density of peaks in the diffraction pattern therefore decreases the preparation of Cu–Zn alloy, which increases pickle size by means of the mechanical mill in the due to reduced size and increased lath stress. Alloy Cu<sub>60</sub>Zn<sub>40</sub> was formed in optimal conditions after 10 hours of frying. The alloy is lent with the decrease in temperature because the Cu–Zn method's mixing enthalpy is negative.

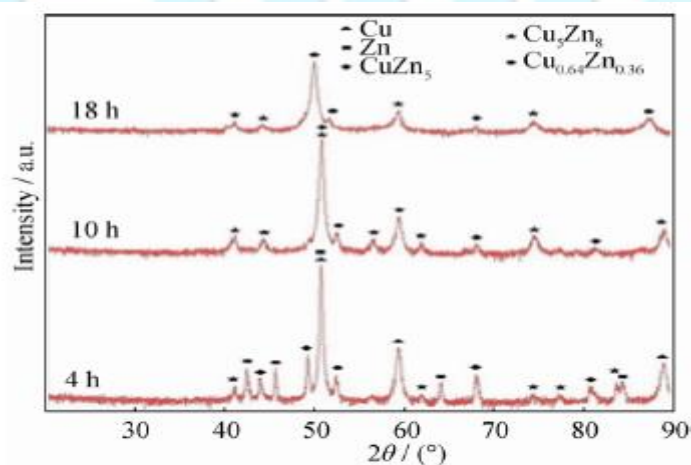


**Figure: XRD patterns of Cu<sub>60</sub>Zn<sub>40</sub> after different durations of mechanical alloying.**

This graph is presented as a lattice strain vs mechanical time alloy. With increasing mechanical alloys, the stress of the crystalline grid has continuously increased and reached 51% after 18 hours. Fracture and grain rotation are expected to cause stress as the dominant methods in the mechanical friction process. In addition to decreased dissemination activation energy, increased grid pressure and dislocation density lead to longer, broad-spectrum routes.

### SEM and EDX analyses

In SEM images of Cu–Zn and Cu-00Zn–Al<sub>2</sub>O<sub>3</sub>, which appear after 18 hours of mechanical fraying, these figures show the differences in the morphology and size of powders before and after fraying. After 18 hours of mechanical alloys, the form of these particules is irregular. The average particle size varies between 10 and 50 μm. Differences in morphology and powder size result from the diffusion of zinc and alumina copper particles during frying.

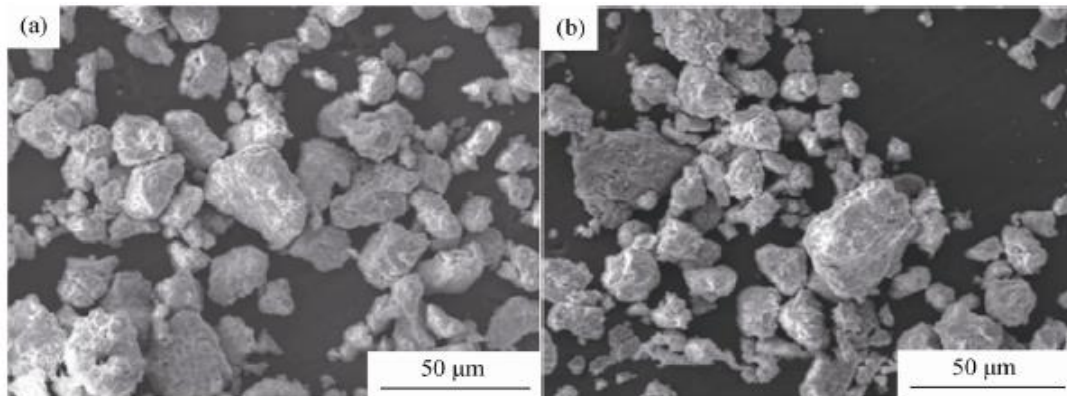


Figure: Morphologies of (a) Cu–Zn and (b) Cu–Zn–Al<sub>2</sub>O<sub>3</sub> powder after 18 h of milling.

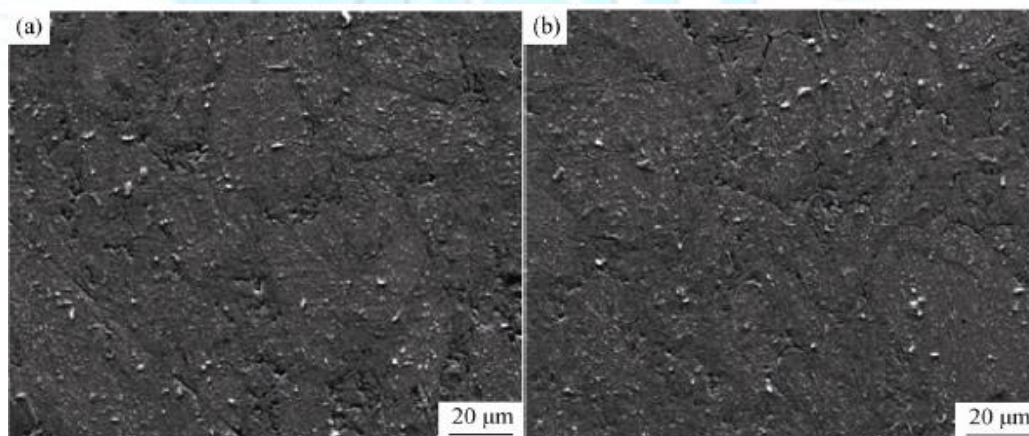


Figure: SEM images of the cross-sectional microstructure of sintered samples: (a) Cu–Zn alloy and (b) Cu–Zn–Al<sub>2</sub>O<sub>3</sub>nanocomposite.

We found that the copper matrix uniformly distributes aluminum and zinc components. The formation of the nanocomposite Cu–Zn–Al<sub>2</sub>O<sub>3</sub> is thus confirmed. Others reported similar results

### Hardness results

The total value of the five Vicker hardness measurements for the materials of Cu–Zn alloy and Cu–Zn–Al<sub>2</sub>O<sub>3</sub> nanocomposite is HV1 244 and 283, respectively. The tests show that 5 volts of Nanoparticles were of an extra hardness 15% higher than those of aluminum. The uniform distribution of hard alumina nanoparticles, according to the results of the same research, hampers the plastic formation of the Cu–Zn matrix under load and increases durability, because it lowers the hardness. The hardness of single hard alumina parts, estimated to have an approximate hardness of approximately HV1 1800, is attributable to the dispersal hardness effects. The mechanical action takes place when strengthening parts in the matrix are nanometric in scale and copper alumina in volumes by mechanical alloy are less than 15 volts percent and the effect on hardness is examined by the additive Their results have demonstrated an increase in volume.

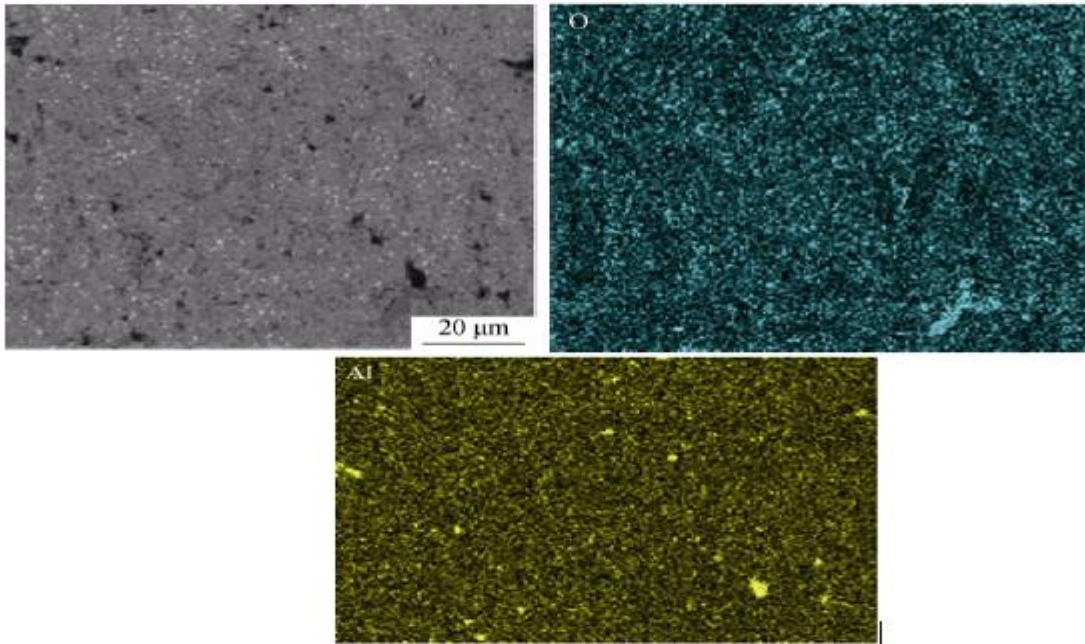


Figure: EDS distribution maps of Zn, O, Al, and Cu for the Cu-Zn-Al<sub>2</sub>O<sub>3</sub> nanocomposite

Table: Density of the Cu-Zn alloy and the Cu-Zn-Al<sub>2</sub>O<sub>3</sub> nanocomposite

Sample	Green density / %	Sintered density / %
Cu-Zn	73	89
Cu-Zn-Al <sub>2</sub> O <sub>3</sub>	75	94

The weight loss of the Cu-Zn and Cu-Zn-Al<sub>2</sub>O<sub>3</sub> nanocomposites is 0.73 mg and Cu-Zn-Al<sub>2</sub>O<sub>4</sub> mg , respectively. A weight loss for the wear test is 40% reduced by the presence of aluminum nanoparticles in the nanocomposite. In the same way, other studies have shown that the wear rate in the aluminum-based alloy decreases from 4.5 to 2.5 g N<sup>-1</sup> · m<sup>-1</sup> with an additive of 5 vol%, the wear rates for the copper-based allocation decreased from 4.5 to 2.5 g. The wear rate of the aluminum reinforcement nanoparticles in the copper-zinc matrix has been reduced as clarified

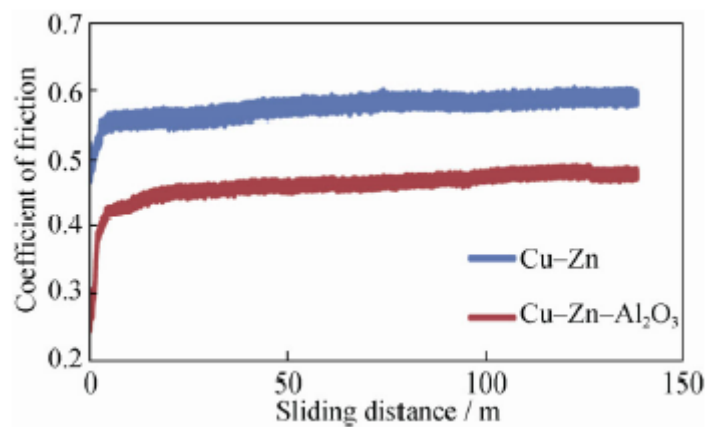
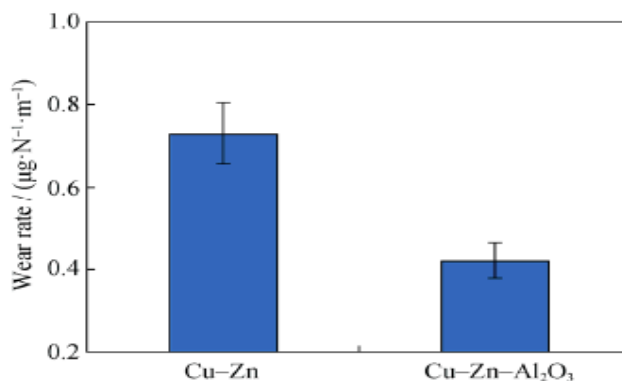


Figure: Coefficients of friction for the Cu-Zn alloy and the Cu-Zn-Al<sub>2</sub>O<sub>3</sub> nanocomposite sintered samples.



**Figure:** Wear-rate data from wear tests for the Cu-Zn alloy and the Cu-Zn-Al<sub>2</sub>O<sub>3</sub> nanocomposite.

The Cu-Zn-Al<sub>2</sub>O<sub>3</sub> nanocomposite corresponds to the lowest COF level. The presence of nanoparticles therefore affects the efficiency and tribology of Cu-Zn alloy significantly. The uniform distribution of nanoparticles in a metal matrix results in a higher hardness, by restricting dislocation movement and flattening.

#### Immersion tests

The effect of additional nanoparticles on Cu-00Zn corrosion properties was investigated using 336 hour immersion tests with 3.5 % NaCl solution. Corrosive diagnostics tests such as H<sub>2</sub>O, O<sub>2</sub> and chloride ion, resulting in reduced adhesive bond stability and increased sintered reaction speeds, and hence sintered part destruction. The Open Circuit Potential (OCP) values are illustrated in the figure. As shown in this figure, OCP values for both samples decreased with increasing immersion time and changed to more active (cathodic) direction.

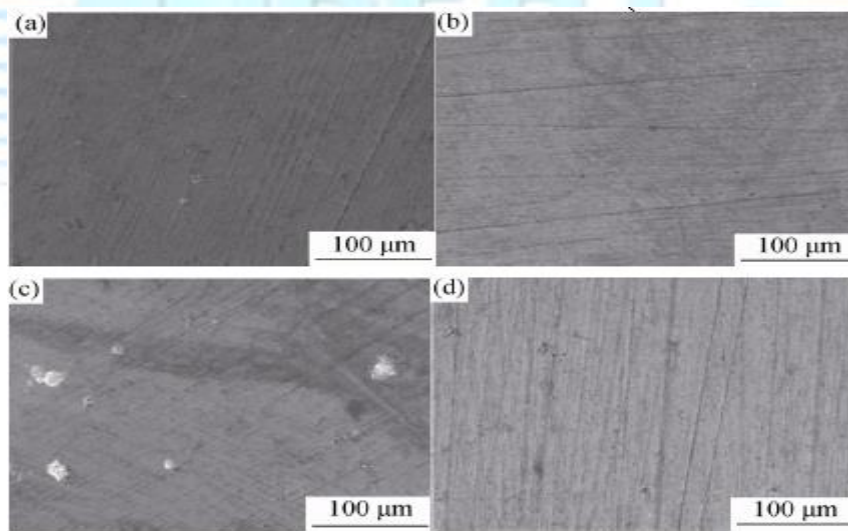


**Figure:** SEM images of the corroded surfaces obtained from immersion tests in a 3.5wt% NaCl solution at different times: Cu-Zn alloy at (a) 12 h, (c) 48 h

The copper zinc alloy was prepared in this analysis after 18 hours of mechanical frying. With the addition of Alumina nanoparticles in the Cu-Zn alloy, the total friction-coefficient (COF) and weight loss levels have decreased by 20 percent and 40 % respectively. The aluminum nanoparticles changed the wearing process in the Cu-Zn alloy matrix from adhesive to abrasive. The current rate of corrosion of Cu-Zn-Al<sub>2</sub>O<sub>3</sub> alloy for Cu-Zn is 90 percent lower. As a result, aluminum nanoparticles were present in the alloy, the corrosion current of the Alloy fell significantly.

#### Conclusion:

In this study, after 6 pm of mechanical frying the copper-zinc alloy was prepared. The coefficient of friction and weight loss rates of 20 percent and 40% decreased, respectively, by the addition of aluminum nanoparticles into the Cu-Zn alloy. The wear mechanisms have been changed in the Cu-Zn alloy matrix from adhesive to abrasive. The Cu-Zn-Al<sub>2</sub>O<sub>3</sub> corrosion current density is 90 percent lower than the Cu-Zn alloy density. The presence of alumina nanoparticles in the alloy thus led to a significant decrease in alloy corrosion current. The

corrosion rate of the Cu–Zn–Al<sub>2</sub>O<sub>3</sub> nanocomposite specimen shows that the micrographs obtained from immersion tests is less than the Cu–Zn Alloy.

**References:**

- [1]. M.F. Zawrah, H.A. Zayed, R.A. Essawy, A.H. Nassar, and M.A. Taha, Preparation by mechanical alloying, characterization and sintering of Cu and 20wt.% Al<sub>2</sub>O<sub>3</sub> nanocomposites, *Mater. Des.*, 46(2013), p. 485.
- [2]. V. Rajković, D. Božić, M. Popović, and M.T. Jovanović, The influence of powder particle size on properties of Cu–Al<sub>2</sub>O<sub>3</sub> composites, *Sci. Sintering*, 41(2009), p. 185
- [3]. K. Jach, K. Pietrzak, A. Wajler, A. Sidorowicz, and U. Brykała, Application of ceramic preforms to the manufacturing of ceramic-metal composites, *Arch. Metall. Mater.*, 58(2013), No. 4, p. 1425
- [4]. S.K. Pabi and B.S. Murty, Mechanism of mechanical alloying in Ni Al and Cu Zn systems, *Mater. Sci. Eng. A*, 214(1996), No. 1-2, p. 146.
- [5]. M. Korać, Z. Anđić, M. Tasić, and Ž. Kamberović, Sintering of Cu–Al<sub>2</sub>O<sub>3</sub> nano-composite powders produced by a thermochemical route, *J. Serb. Chem. Soc.*, 72(2007), No.11, p. 1115.
- [6]. F. Shehata, M. Abdel hameed, A. Fathy, and M. Elmahdy, Preparation and characteristics of Cu–Al<sub>2</sub>O<sub>3</sub> nanocomposite, *Open J. Met.*, 1(2011), p. 25.
- [7]. P.Suresh, D.V.Sreekanth, A P Arun Pravin, D.Soundarrajan, " Numerical Analysis of Savonius Wind Turbine Using Fluid Dynamics", *International Journal for Research in Applied Science & Engineering Technology*, Vol-7, Issue-1, Jan-2019, PP-159-164.

